Model Order Reduction of Aeroservoelastic Model of Flexible Aircraft

Yi Wang[1], Hongjun Song[2], Kapil Pant [3]
CFD Research Corporation, Huntsville, AL 35806

and

Martin J. Brenner[4], Peter Suh[5]
NASA Armstrong Flight Research Center, Edwards, CA 93523

This paper presents a holistic model order reduction (MOR) methodology and framework that integrates key technological elements of sequential model reduction, consistent model representation, and model interpolation for constructing high-quality linear parameter-varying (LPV) aeroservoelastic (ASE) reduced order models (ROMs) of flexible aircraft. The sequential MOR encapsulates a suite of reduction techniques, such as truncation and residualization, modal reduction, and balanced realization and truncation to achieve optimal ROMs at grid points across the flight envelope. The consistence in state representation among local ROMs is obtained by the novel method of common subspace reprojection. Model interpolation is then exploited to stitch ROMs at grid points to build a global LPV ASE ROM feasible to arbitrary flight condition. The MOR method is applied to the X-56A MUTT vehicle with flexible wing being tested at NASA/AFRC for flutter suppression and gust load alleviation. Our studies demonstrated that relative to the full-order model, our X-56A ROM can accurately and reliably capture vehicles dynamics at various flight conditions in the target frequency regime while the number of states in ROM can be reduced by 10X (from 180 to 19), and hence, holds great promise for robust ASE controller synthesis and novel vehicle design.

Nomenclature

A	=	state matrix
A_m	=	state matrix in the modal form
B	=	input matrix
C	=	output state matrix
D	=	input transition
$\hat{L}$	=	accumulative transformation matrix
M	=	matrices in state space model
P	=	controllability gramian
p	=	pitch rate
Q	=	observability gramian
q	=	pitch rate
R	=	common subspace for reprojection
r	=	yaw rate
T	=	transformation matrix for consistent state representation
$\hat{L}$	=	accumulative transformation matrix
u	=	input signals
y	=	response measurements
$\tilde{V}$	=	transformation matrix in balanced realization

[1] Director, CFD Research Corporation, AIAA Member; yi.wang@cfdrc.com

[2] Principal Research Engineer, CFD Research Corporation, non AIAA Member; hongjun.song@cfdrc.com

[3] Vice President, CFD Research Corporation, non AIAA Member; kapil.pant@cfdrc.com

[4] Aerospace Engineer, Aerostructures Branch, and AIAA Senior Member; martin.j.brenner@nasa.gov

[5] Aerospace Engineer, Aerostructures Branch, and AIAA Member; peter.m.suh@nasa.gov

$\tilde{W}$	=	transformation matrix in balanced realization
W	=	weights for matrix interpolation
ρ	=	a vector of measurable parameters
Λ	=	diagonal blocks of the eigenvalue magnitude in the modal form
Ω	=	Matrix for modal form transformation

I.   Introduction

The flight performance of aerospace systems is characterized by the interaction between aerodynamics, structural dynamics, and flight control dynamics. Modern designs of aerospace vehicles utilize state-of-the-art materials and flexible structures that are lightweight and low-cost to achieve better maneuverability, and high performance. As the structures become progressively lighter and more flexible, they are prone to complex dynamics, stability and durability issues. In addition, the control systems interactions with aerodynamic and structural nonlinearities can result in instabilities such as flutter [1], limit cycle oscillations (LCO) [2], and gust loads [3], leading to unacceptable flight conditions and risk to the mission. Modeling, and especially maneuvering simulation, of high-order aeroservoelastic (ASE) systems is essential for successful development of relatively lightweight, necessarily flexible, aircraft with complex unsteady and often nonlinear aerodynamics. Therefore, the ability to accurately predict aeroelastic (AE) behavior in conjunction with control law design of sensors and actuators is essential for developing high-performance, safe aerospace vehicles. Although high-fidelity simulation coupling the nonlinear aerodynamics with structural models enables a direct insight into the aforementioned phenomena, its prohibitive computational cost, speed mismatch, nonlinear nature, as well as difficulty to deploy controllers with high-state-order models render it impractical for integration in the design environment involving concurrent ASE analysis and control synthesis and design.

To address these challenges, a variety of model order reduction (MOR) techniques have been developed in conjunction with the linear parameter varying (LPV) formulation to reduce high-order aircraft ASE model into a reduced state-space form while retaining dominant dynamics of the system. In LPV, the fully coupled nonlinear aircraft model is represented as an ensemble of linear models of which the system parameters vary across the flight regime. The landmark efforts in the area include regular truncation and residualization [4], modal reduction [5], balanced realization and truncation [4, 5], Krylov-based projection and the hybrid SVD-Krylov approach [6]. MOR approaches based on model transformation and truncation, such as modal reduction, balanced realization, and Krylov projection lead to different state representation of the reduced models at various parameter locations in the flight envelope, and hence, they cannot be immediately interpolated. In order to interpolate reduced models to form global LPV models encompassing the entire flight envelope, various model transformation techniques have been proposed to achieve consistent state representation among local reduced models prior to interpolation. Hjartarson et al. [4] developed an LPV aeroservoelastic control toolbox (LPVtools), which was used to derive the reduced state-space form of a grid-based LPV model of aircraft. In their approach, the transformation matrix obtained from balanced realization at a single flight condition was applied across the entire flight envelope to preserve consistent state presentation (but at the cost of non-optimal reduction performance). Moreno et al [7] exploited the coprime factorization approach in conjunction with the balanced realization to attain a low-order, control-oriented LPV Body Freedom Flutter (BFF) model with 26 states consistent across the flight domain, and identify the numerical issues of the approach associated with the high state orders. Panzer et al. [8] proposed two methods, respectively, based on reprojection into a common subspace and optimization-based matrix matching to achieve identical state meanings among local models for interpolation. The former was employed for interpolating LPV reduced models of industrial flexible aircraft [6]. Recently Theis et al [5] developed another modal matching technique, which essentially determines a mode-wise canonical form and matches modes with similar dynamic properties at neighboring grid points to minimize the approximation error due to state inconsistency.

This paper presents the development of LPV ASE reduced order models (ROMs) of flexible aircrafts based on a combination of sequential model order reduction (MOR), consistent model representation, and model interpolation approaches. The sequential MOR encapsulates a suite of reduction techniques, such as traditional truncation and residualization, modal reduction, and balanced realization and truncation, and is applied to the X-56A MUTT vehicle with flexible wing developed by Lockheed Martin and currently being tested at NASA/AFRC for flutter suppression and gust load alleviation. The traditional truncation and residualization methods are first conducted on the states of the sensors, actuators, aerodynamic lags, rigid bodies, elastic structures of the full-order X-56A MUTT ASE model sequentially. The transformation-based MOR including modal reduction and balanced realization and truncation is then performed to further refine the frequency contents and remove the states with small contribution to the input/output energy of the system in the local reduced model. Next, the method of reprojection into a common

subspace is utilized to remedy the issue of inconsistent state representation among the local reduced models caused by the flight condition-dependent transformation above, which allows model interpolation in the reduced domain and results in a unified LPV ROM applicable across the entire flight envelope. The input/output behavior and the system response of the original and the ASE ROMs of the X-56A is compared in the frequency domain.

II. Linear Parameter-Varying Aeroservoelastic Models of Aircraft

Linear parameter-varying (LPV) models are state-space models whose state-space descriptions are functions of time-varying parameters, i.e.,

$$\begin{bmatrix} \dot{x} \\ y \end{bmatrix} = \begin{bmatrix} A(\rho) & B(\rho) \\ C(\rho) & D(\rho) \end{bmatrix} \begin{bmatrix} x(t) \\ u(t) \end{bmatrix} \tag{1}$$

where $A(\rho)$ is the state matrix, $B(\rho)$ is the input matrix, $C(\rho)$ is the output state matrix, $D(\rho)$ is the input transition matrix, $\rho \in \mathfrak{R}^{np}$ is a vector of measurable parameters (such as altitude, Mach, fuel weight, etc.), $u \in \mathfrak{R}^{nu}$ and $y \in \mathfrak{R}^{ny}$ are, respectively the vector of the control input and measurement. There are several methods to represent the parameter dependence in LPV models above, such as linear fractional transformation, polytopic dependence of the state matrix on the parameters, linearization on a gridded domain, etc. This paper targets the MOR of LPV models based on the gridded domain to agree with the full-order X-56A models. The gridded domain LPV is illustrated in Figure 1, in which the nonlinear dynamics in the ASE problem of the aircraft is treated as its linearization around various flight operating points (also termed grid points or parameter locations hereafter). A set of original, full-order Linear Time Invariant (LTI) state space models are first constructed at the grid points in the domain, and then can be used for ROM generation and controller synthesis.
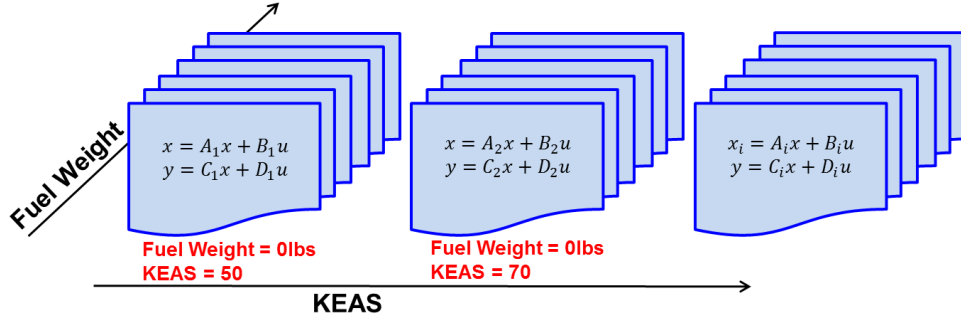

Figure 1. linear parameter varying (LPV) formulation of the aeroservoelastic (ASE) models of aircraft

III. Model Order Reduction for LPV Aircraft Models

Figure 2 illustrates our MOR methodology for LPV ASE models of aircraft. A prerequisite of the approach to construct LPV ROMs is to first have a set of full-order LTI state space models describing coupled ASE and flight control behavior at grid points in the parameter space. The full model can be generated from various relevant modeling tools (e.g., ZAERO [9], NASTRAN [10] or others) as shown in the blue box in Figure 2a. The entire MOR process includes two steps: (1) **Local MOR** (red box in Figure 2a): the full-order LTI model set is first reduced and transformed onto a low-dimension subspace to generate a set of local ROMs. Several techniques can be used, including truncation and residualization, transformation and truncation (e.g., modal reduction and balanced realization and truncation, Krylov methods, and their combinations); and (2) **Model Interpolation and PV ROM Realization** (green box): the global LPV ROM applicable to the entire flight envelope is obtained by interpolating the system matrices of the local ROM set obtained in the previous step. As the transformation used in step (1) depends on the location of the grid points, measures need to be taken to ensure all the ROMs are cast in a consistent state representation (or coordinates) prior to model interpolation. Eq. (2) summarizes the MOR process

$$\begin{bmatrix} \dot{x} \\ y \end{bmatrix} = \begin{bmatrix} A_i & B_i \\ C_i & D_i \end{bmatrix} \begin{bmatrix} x(t) \\ u(t) \end{bmatrix} \xrightarrow[\substack{\text{Consistent State} \\ \text{Represenation}}]{MOR} \begin{bmatrix} \dot{x}_i^* \\ y \end{bmatrix} = \begin{bmatrix} A_i^* & B_i^* \\ C_i^* & D_i^* \end{bmatrix} \begin{bmatrix} x_i^* \\ u(t) \end{bmatrix} \xrightarrow[\text{Varying}]{Parameter} \begin{bmatrix} \dot{x}^* \\ y \end{bmatrix} = \begin{bmatrix} A_{PV}^*(\rho) & B_{PV}^*(\rho) \\ C_{PV}^*(\rho) & D_{pV}^*(\rho) \end{bmatrix} \begin{bmatrix} x^* \\ u(t) \end{bmatrix} \tag{2}$$
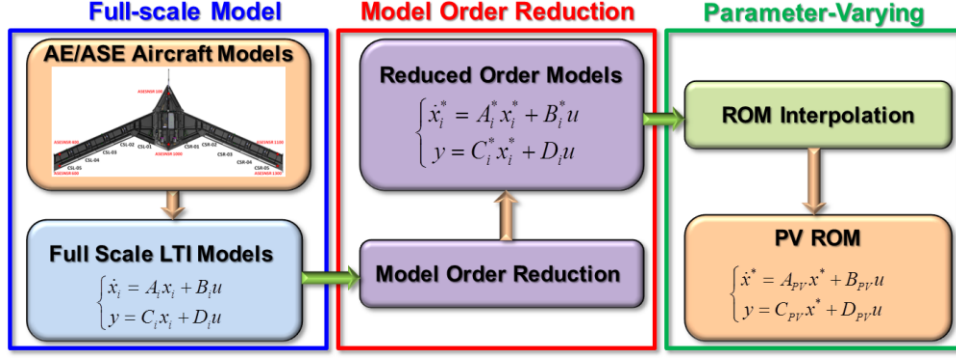
Figure 2. Organization of linear parameter varying (LPV) model order reduction (MOR) framework

Three MOR techniques have been developed in our framework for the local MOR process, namely, truncation and residualization, modal reduction, and balanced truncation. The approach of reprojection into common subspace and the linear model interpolation are used, respectively, for consistent state representation and LPV ROM across the flight envelope. They are presented in the following sections:

A Truncation and Residualization

MOR by truncation and residualization essentially partitions the state vector x in the model into two components $[x_1 \ x_2]^T$, where x_1 are the states to keep and x_2 are those to eliminate. Therefore the system matrices, A, B, and C can be partitioned as:

$$A = \begin{bmatrix} A_{11} & A_{12} \\ A_{21} & A_{22} \end{bmatrix}, \quad B = \begin{bmatrix} B_1 \\ B_2 \end{bmatrix}, \quad C = \begin{bmatrix} C_1 & C_2 \end{bmatrix} \tag{3}$$

The ROM is obtained by truncating all the terms associated with x_2. Truncation preserves the ROM accuracy at high frequencies. When the steady state gain of a system needs to be retained, a residualization procedure is implemented, in which the state derivatives for x_2 are set to zero, leading to a more accurate approximation of the original system at low frequency. The residualized ROM is then given by,

$$\begin{bmatrix} \dot{x}_1 \\ y \end{bmatrix} = \begin{bmatrix} \left(A_{11} - A_{12}A_{22}^{-1}A_{21}\right) & \left(B_1 - A_{12}A_{22}^{-1}B_2\right) \\ \left(C_1 - C_2A_{22}^{-1}A_{21}\right) & \left(D - C_2A_{22}^{-1}B_2\right) \end{bmatrix} \begin{bmatrix} x_1(t) \\ u(t) \end{bmatrix} \tag{4}$$

B Modal Reduction

Modal reduction relies on the real and ordered eigenstructure decomposition to cast the full-order model into a modal realization form before state truncation. The modal realization form transforms the state matrix A into a block diagonal form A_m with either 1X1 or 2X2 blocks when the eigenvalue is real or complex, respectively [11]. That is, $\Omega^{-1}A\Omega = A_m$, were Ω is a set of "real" eigenvectors spanning the same eigenspace as the complex ones, which leads to

$$\begin{bmatrix} \dot{x}_m \\ y \end{bmatrix} = \begin{bmatrix} A_m & B_m \\ C_m & D \end{bmatrix} \begin{bmatrix} x_m(t) \\ u(t) \end{bmatrix} \tag{5}$$

where the system matrices in the modal realization are given by

$$A_m = \begin{bmatrix} \Lambda_r & 0 \\ 0 & \Lambda_{n-r} \end{bmatrix}, \quad B_m = \Omega^{-1}B, \quad C_m = C\Omega \tag{6}$$

The diagonal blocks Λ are normally arranged in ascending order according to their eigenvalue magnitude. The magnitude of a complex eigenvalue (for an oscillatory mode) is its angular frequency, while for a real eigenvalue, it is the damping coefficient. Then a threshold magnitude can be set to partition Λ in A_m into Λ_r and Λ_{n-r}. All the states associated with Λ_r will be retained (with those for Λ_{n-r} truncated) to capture the frequency range of interest for control design.

C Balanced Realization and Truncation

Balanced truncation relies on the balancing transformation to determine minimal realization of the model based on the Hankel singular values. The controllability and observability gramians of the LTI model above is given by

$$AP + PA^T + BB^T = 0 \quad \text{and} \quad A^T Q + QA + C^T C = 0 \tag{7}$$

The balancing transformation matrix then can be calculated as:

$$\tilde{V} = UZ\Sigma^{-1/2} \quad and \quad \tilde{W} = LY\Sigma^{-1/2} \tag{8}$$

where $P = UU^T$ and $Q = LL^T$ and Z, Σ, and Y can be obtained from singular value decomposition $U^T L = Z\Sigma Y^T$. Applying the balancing transformation to the state-space model yields,

$$\begin{bmatrix} \dot{x}_b \\ y \end{bmatrix} = \begin{bmatrix} \tilde{W}^T A \tilde{V} x_b & \tilde{W}^T B \\ C\tilde{V} & D(\rho) \end{bmatrix} \begin{bmatrix} x(t) \\ u(t) \end{bmatrix} \tag{9}$$

The state-space model in the new coordinate in Eq. (9) is balanced, and hence, its controllability and observability gramians are equal and diagonal, i.e., $P_b = Q_b = \text{diag}(\sigma_1, \ldots, \sigma_r \ldots, \sigma_n)$, where $\sigma_1, \ldots, \sigma_n$ are the Hankel singular values sorted in descending order. By removing the states corresponding to low Hankel singular values (e.g., $\sigma_{r+1} \ldots \sigma_n$), a ROM without appreciably losing important input/output energy can be obtained. Note that balanced realization and truncation only applies to stable systems, although the aircraft state-space model may include unstable states. In order to circumvent this issue, typically a stable/unstable state partitioning needs to be performed prior to the balanced truncation.

The aforementioned ROM steps are applied to the full-order state-space model of the aircraft at each grid point in the flight envelope, yielding a set of local ROMs

$$\begin{bmatrix} \dot{\hat{x}}_{r,i} \\ y \end{bmatrix} = \begin{bmatrix} \hat{A}_{r,i} & \hat{B}_{r,i} \\ \hat{C}_{r,i} & D_i \end{bmatrix} \begin{bmatrix} \hat{x}_{r,i}(t) \\ u(t) \end{bmatrix} \tag{10}$$

where i denotes the ith grid point in the parameter space, $\hat{A}_{r,i} = \hat{L}_i A_i \hat{U}_i$, $\hat{B}_{r,i} = \hat{L}_i B_i$, and $\hat{C}_{r,i} = C_i \hat{U}_i$ are the system matrices of ROM at the ith grid point following the modal and balanced transformation. A_i, B_i, and C_i are the system matrices obtained only through truncation and residualization (without state transformation). $\hat{L}_i$ and $\hat{U}_i$ are the accumulative transformation matrix derived from Ω, $\tilde{W}$, and $\tilde{V}$.

The next step is to interpolate the ROM computed at the grid points to obtain a global LPV ROM that can be used for controller design at arbitrary locations in the parameter space. Due to different transformation matrices used in MOR (e.g., modal reduction and balanced truncation), the states of the reduced state space model have different physical meanings and are not consistent across the flight envelope. Therefore, the ROM cannot be interpolated directly.

D Reprojection onto Common Subspace

One of the most effective methods to resolve the issue above is to project the individual ROM at grid points in the parameter space onto a common basis (subspace), followed by matrix interpolation as discussed in [8]. However the method in [8] requires the transformation matrix to be orthonormal, and hence, is not immediately applicable to transformation matrices ($\hat{U}_i$ in Eq. (10)) computed from the modal reduction and the balanced truncation. Therefore, an additional coordinate transformation G_i is needed to yield a ROM set spanned by orthonormal bases prior to reprojection. Taking an SVD on transformation $\hat{U}_i$ matrix above yields

$$\hat{U}_i = V_i S_i Y_i^T, G_i = S_i Y_i^T \tag{11}$$

Applying transformation G_i (i.e., $x_{r,i} = G_i \hat{x}_{r,i}$) to Eq. (10) leads to another set of ROMs with new states $x_{r,i}$, which has the same dimension as $\hat{x}_{r,i}$ but with an orthonormal projection matrix V_i, i.e.,

$$\begin{bmatrix} \dot{x}_{r,i} \\ y \end{bmatrix} = \begin{bmatrix} A_{r,i} & B_{r,i} \\ C_{r,i} & D_i \end{bmatrix} \begin{bmatrix} x_{r,i}(t) \\ u(t) \end{bmatrix} \quad \text{where} \quad A_{r,i} = W_i^T A_i V_i, \quad B_{r,i} = W_i^T B_i, \quad C_{r,i} = C_i V_i \tag{12}$$

where $W_i^T = G_i \hat{L}_i$. Given orthonormal V_i, the procedure of common subspace reprojection can be undertaken. Given $x_i = V_i x_{r,i}$ (see Eq. (12)), a linear projection matrix R can be defined which is common to all local ROMs at grid points, such that $x_i^* = R^T x_i$ to force the projected states x_i^* of the local states to be equal, that is

$$R^T V_1 x_{r,1} = R^T V_2 x_{r,2} = \ldots = R^T V_{n_s} x_{r,n_s} = x_i^* = x^* \tag{13}$$

Thus the transformation from x^* to $x_{r,i}$ can be expressed as $x_{r,i} = T_i^{-1} x^*$, where $T_i = R^T V_i$. Thus the new ROMs at the grid points with consistent state representation is given by

$$\begin{bmatrix} \dot{x}_i^* \\ y \end{bmatrix} = \begin{bmatrix} A_i^* & B_i^* \\ C_i^* & D_i \end{bmatrix} \begin{bmatrix} x_i^*(t) \\ u(t) \end{bmatrix} \quad \text{where} \quad A_i^* = T_i A_{r,i} T_i^{-1}, \quad B_i^* = T_i B_{r,i}, \quad C_i^* = C_{r,i} T_i^{-1} \tag{14}$$

The transformation matrix R should capture most transformation information V_i of the local models at the grid points. Therefore a straightforward choice for R is to take the underlying basis of all V_i using SVD and truncation, that is,

$$RS\Phi^T \approx \begin{bmatrix} V_1, & \dots & V_{n_s} \end{bmatrix} \tag{15}$$

Once Eq. (14) for all grid points becomes available, they can be interpolated to obtain LPV ROM that is applicable at an arbitrary location in the parameter space. Typical interpolation approaches include (1) polynomial regression of the matrix elements A_i^* using the values at the local models; and (2) matrix interpolation. The second approach was used in this paper, which is described by

$$M^* = \sum_{i=1}^{s} w(\rho) M_i^* \tag{16}$$

where M_i^* is the A_i^*, B_i^*, C_i^*, and D_i^*, at the grid point i. and s is the number of the grid points surrounding the parameter location ρ. $w(\rho)$ is the weights for interpolation at location ρ, and a linear weight inversely proportional to the distance between ρ and grid points i was used in this paper.

IV. X-56A MUTT Model

The LTI state-space models of the X-56A MUTT airframe were provided by NASA/AFRC. They were developed using the generalized mass, stiffness, and aerodynamic matrices obtained by MSC/Nastran [10] and ZAERO [9]. There are 10 control surfaces on the vehicle, five on each wing; and 2 throttle controls for engine dynamics as shown in Figure 3. The five actuators on the left wing are labeled as BFL, WF1L, WF2L, WF3L, and WF4L starting from the inner body to the outer wing tip. Likewise, the actuators on the right wing are labeled as BFR, WF1R, WF2R, WF3R, and WF4R based on the same convention above. The rigid-body state sensors (IMU-MIDG) are located around the center of the vehicle, while the six accelerometer locations are, respectively, placed at the front of the vehicle (ASESNSR100), at the rear (ASESNSR1000), at the leading and trailing edge of the left wing (ASESNSR400 and ASESNSR600), and of the right wing (ASESNSR1100 and ASESNSR1300).
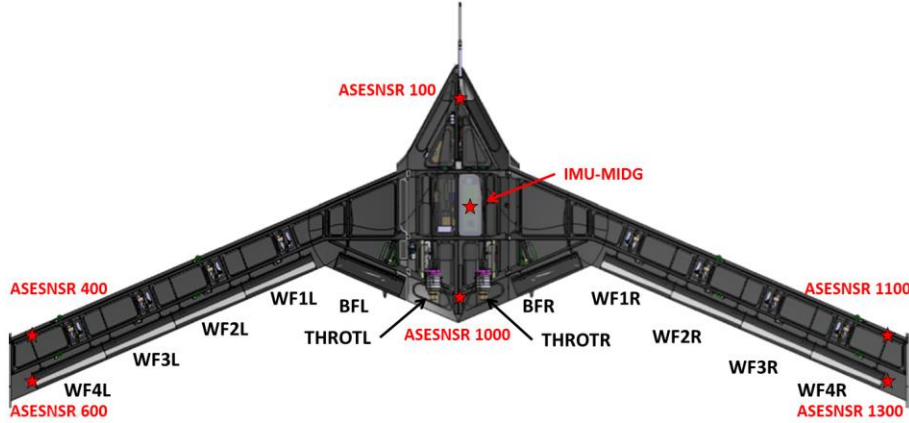

Figure 3. Sensors and actuators deployment in the X-56A MUTT vehicle

A set of 495 models were generated at $M = 0.16$ on grid points of a 2D parameter space across the flight envelope. The two parameters are KEAS ("knots equivalent airspeed") and fuel weight, which, respectively, range from 50 KEAS to 150 KEAS in 2 KEAS increments and from 0 lb to 78 lb in 10 lb increments (the last weight has an 8 lb increment). The models have 44 states corresponding to the 2nd-order sensors (22 in total), 12 rigid body states, 14 elastic structural modes and 14 derivatives (modal velocity), 60 aerodynamic lag states, and 36 states for the third order actuators (12 control surfaces). According to the V-g and V-f plots of the X-56A baseline model at $M = 0.16$ [12] the normalized flutter frequencies for SBFF (symmetric body freedom flutter), SWBTF (symmetric wing bending torsion flutter), and AWBTF (anti-symmetric wing bending torsion flutter) modes are, respectively, at 1, 3.68, and 3.912 (that is, all the flutter frequencies are normalized by the one for SBFF). The target normalized frequency range ω for X-56A model reduction is determined to be $0.01 < \omega < 5.36$ to ensure full coverage of the interesting flutter behavior and system response. The sparsity pattern of A matrix is illustrated in Figure 4. The

physical meaning of the states and their corresponding entries in *A* is utilized to guide the MOR process for constructing ROMs. According to [13], the body (BFL and BFR) and the outer most flaps (WF4L and WF4R) are mainly used as control means for stabilization and damping augmentation. Therefore the sensors to be used for observation include the roll (*p*), pitch (*q*), and yaw (*r*) rate sensor, and the accelerometers at the body center (ASESNSR1000) and the trailing edge (ASESNSR600 and ASESNSR1000) of wing tips.

Figure 4. Sparsity pattern and partition of *A* matrix

Figure 5. Flow chart for MOR process and main techniques used in the present effort

For the X-56A state-space model, we used truncation and residualization to eliminate the states associated with sensors, actuators, aerodynamic states, rigid body states, and elastic states, which was followed by transformation-based MOR (modal reduction and balanced realization and truncation). The transformation matrices of the local ROMs are then orthogonalized via SVD and state transformation, and then reprojected onto common subspace to render the model ready for interpolation. Figure 5 summarizes the flow chart of our MOR procedure and the main techniques being used.

V.   Results and Discussion

Case studies were carried out to verify and demonstrate the MOR framework and X-56A ROM. The ROM was compared against the full-order X-56A MUTT state model provided by NASA/AFRC in terms of input/output behavior and system response in the frequency domain. Various aspects of the X-56A ROM were interrogated, including sequential MOR, effects of ROM dimensions, model robustness (or susceptibility to flight parameters), and ROM interpolation. Recall that the body (BFL or bfl_cmd_deg) and the outer most surface controls of the left wing (WF4L or wf4l_cmd_deg) were studied as a control means for stabilization and damping augmentation. The sensors in observation include the roll (*p*), pitch (*q*), and yaw (*r*) rate sensor, and the accelerometers at the body center (ASESNSR1000) and the trailing edge of both wing tips (ASESNSR600 and ASESNSR1300). The full-order X-56A state-space model at the operating condition of 100 KEAS with fuel weight of 10 lbs served as the benchmark/baseline case.

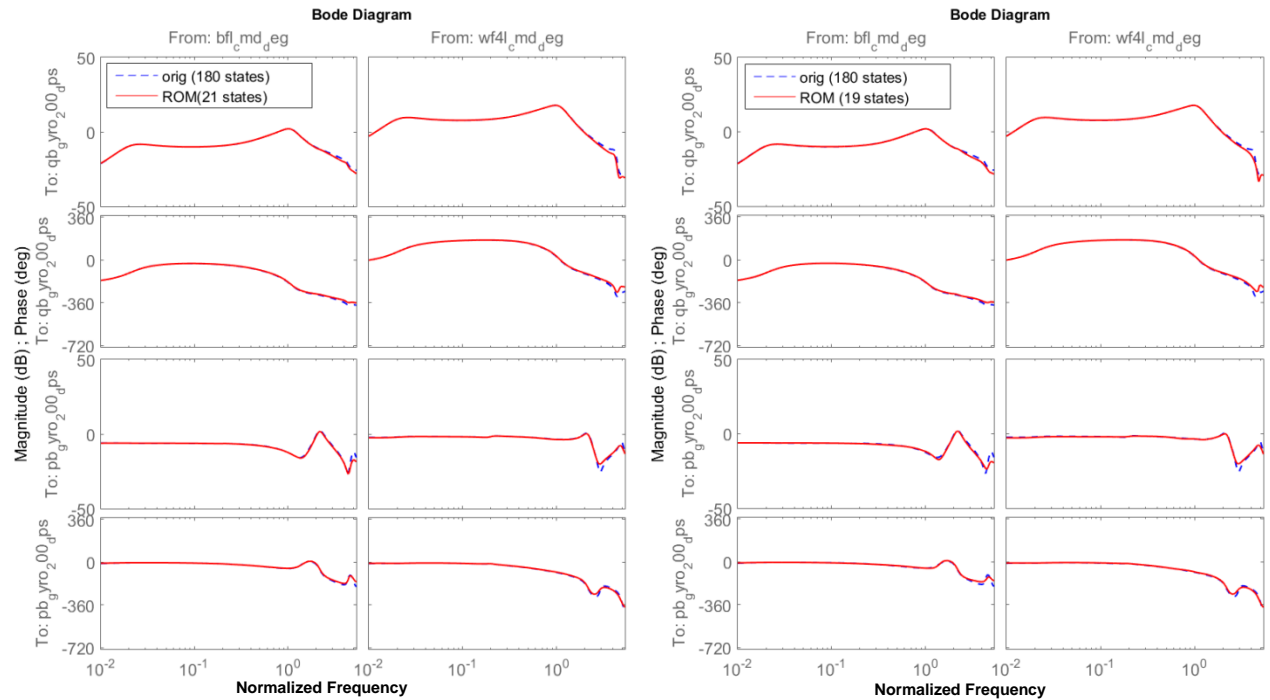### A Sequential Model Order Reduction (MOR)

We first conducted the sequential MOR on the benchmark case following the flow chart in Figure 5. It consists of (1) **sensor reduction**: 32 states of the sensors that are of no interest to observation were truncated. Then the rest 12 states for the sensors in observation were fully residualized to match the DC gain of the full-order model, leading to a local ROM with 136 states; (2) **actuator reduction**: the 30 states corresponding to 10 actuators that are not the object of our ASE study were truncated. The 3rd states of bfl_cmd_deg (BFL) and wf4l_cmd_deg (WF4L) were residualized, leading to 104 states in the model; (3) **aerodynamic lag reduction**: in distinct contrast to the trial-and-error method in the previous work [4] we only retained the first 30 aerodynamic states (out of 60 states) that span a broader frequency range. We relied on the modal reduction step downstream to further filter out unnecessary states at high frequency and refine the ROM. The aerodynamic lag reduction yields a ROM with 74 states; (4) **rigid body state reduction**: the rigid-body states *u*, *h*, *α*, *θ*, *q*, *β*, *p*, *r*, and *ϕ* for the X-56A model were kept in the phugoid mode, which is adequate to generate consistent ROM performance across the entire flight envelope and resolve the dynamic behavior subject to stabilization and damping augmentation. This step results in a ROM with 71 states; (5)

elastic state reduction: the first six elastic states in the modal displacement and modal velocity (12 in total) were retained in the ROM, yielding a ROM of 55 states; (6) **modal reduction**: the 55-state ROM was translated into a block diagonal modal form with eigenvalue sorted in an ascending order according to their magnitudes. 12 states at the high end of the eigenvalue magnitude were truncated, yielding a ROM with 43 states; and (7) **balanced truncation**: through balancing transformation, the states in the model are sorted according to the significance of their corresponding Hankel singular values, 22 states with smaller Hankel singular values were truncated, yielding a ROM with 21 states. There are two salient aspects markedly distinguishing our MOR approaches from prior efforts [4] on X-56A model reduction: (1) instead of applying a single transformation matrix across the entire flight envelope to preserve consistent physical meanings of states among local ROMs, each local ROM in our process was built using the locally optimal transformation. Therefore our local ROM is able to more accurately approximate the original, full-order X-56A state-space models at the grid points; and (2) the method of common subspace reprojection effectively addresses the issue of inconsistent state representation and model interpolation among local ROMs (see Section D below).

The sequential MOR and resulting model sizes are summarized in Table 1. Figure 6a shows the comparison of the magnitude and phase in the frequency domain between the full-order X-56A model and our ROM with 21 states from both inputs BFL (bfl_cmd_deg) and WF4L (wf4l_cmd_deg) to the target outputs, including p (pb_gyro_200_dps), q (qb_gyro_200_dps), r (rb_gyro_200_dps), ASESNSR600 (loaz_200_g), ASESNSR1000 (caz_200_g), and ASESNSR1300 (roaz_200_g). It demonstrates that ROM accurately matches the full-order model for dynamics in all input-output channels within the desired frequency range while the number of states is reduced by almost 10X. This confirms the accuracy and efficiency of our MOR approaches and salient applicability for robust ASE controller synthesis.
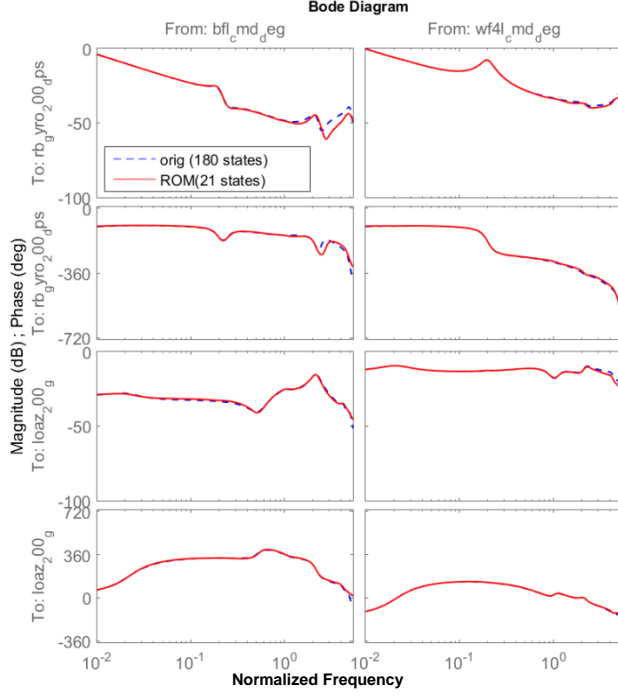
Table 1. Sequential model reduction and resulting model sizes

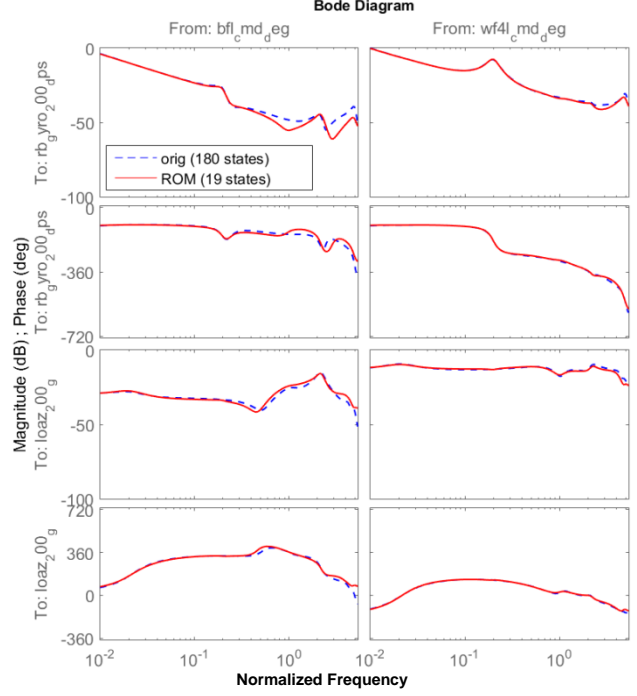| Reduction	Original	Sensor	Actuator	Aerodynamic	Rigid-Body	Elastic	Modal	Balanced Trunc.
Model Size	180	136	104	74	71	55	43	21

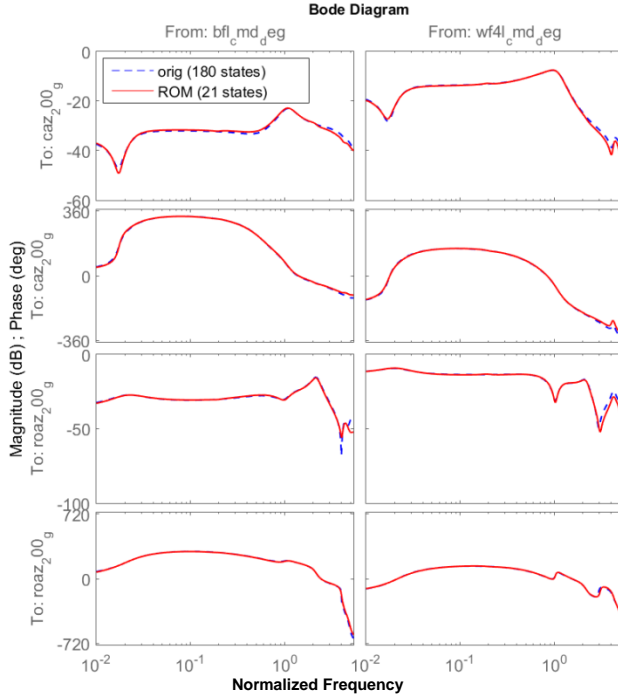**(a-1) From Inputs to q and p**   **(b-1) From Inputs to q and p**
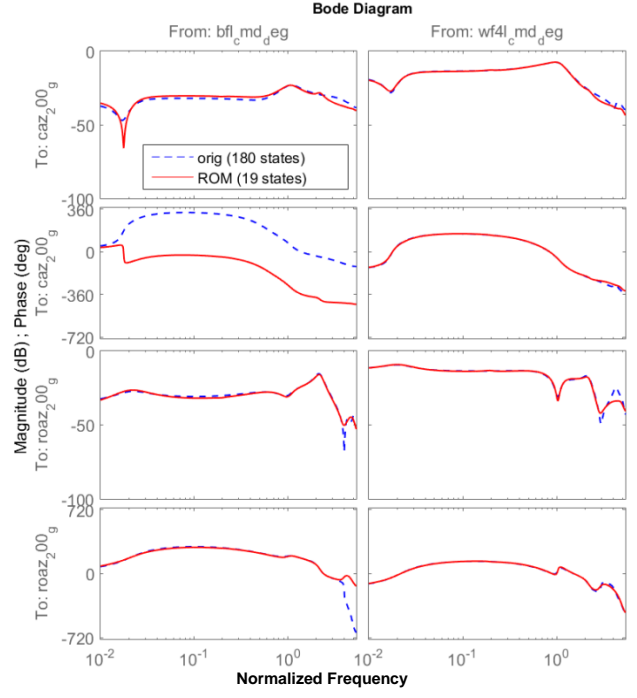
(a-2) From Inputs to r and ASESNSR600

(b-2) From Inputs to r and ASESNSR600

(a-3) From Inputs to ASESNSR1000 and ASESNSR1300

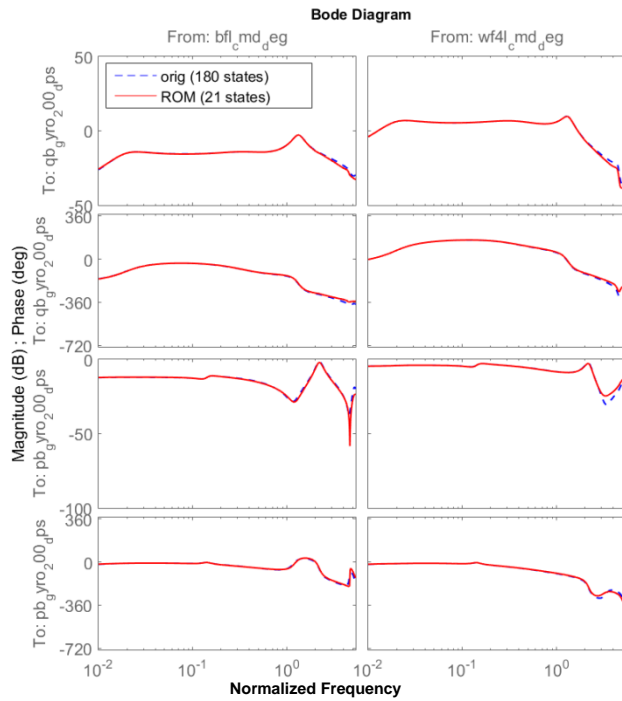**(b-3) From Inputs to ASESNSR1000 and ASESNSR1300**

Figure 6. Comparison in magnitude and phase in the frequency domain between the full-order X-56A model (180 states) and the ROM. From Inputs: bfl_cmd_deg (BFL) and wf4l_cmd_deg (WF4L); To outputs: qb_gyro_200_dps (q), pb_gyro_200_dps (p), rb_gyro_200_dps (r), loaz_200_g (ASESNSR600), caaz_200_g (ASESNSR1000), and roaz_200_g (ASESNSR1300). (a) ROM with 21 states (left panel); and (b) ROM with 19 states (right panel).

9

American Institute of Aeronautics and Astronautics
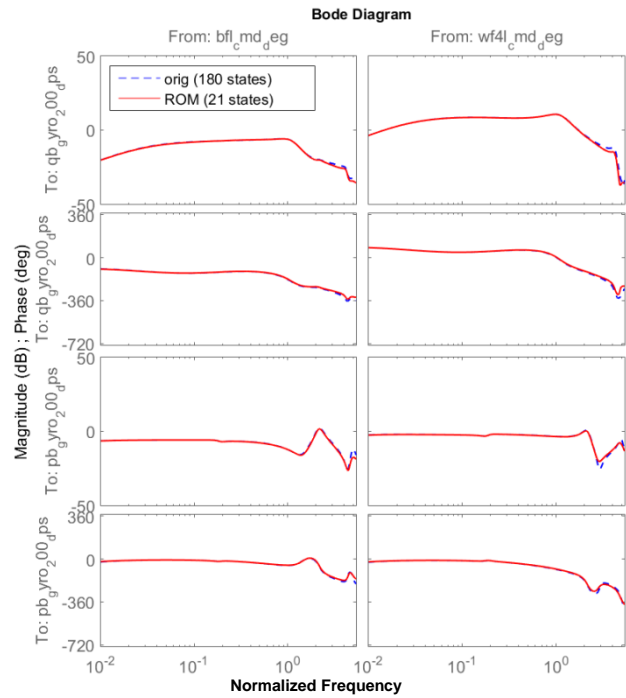
B   Effect of ROM Dimensions

We also carried out a study to investigate the effect of ROM dimensions on the performance in approximating the vehicle dynamics across the frequency range of interest. Specifically, in the balanced truncation above, 24 states with the smallest Hankel single values were truncated, yielding a ROM only with 19 states. Figure 6b shows that even 19-state ROM can predict very well the dynamic behavior among all the input-output pairs, while the discrepancy is more appreciable in the high frequency regime relative to the 21-state ROM. This is within expectation as more controllable and observable information would be lost given lower ROM dimensions.
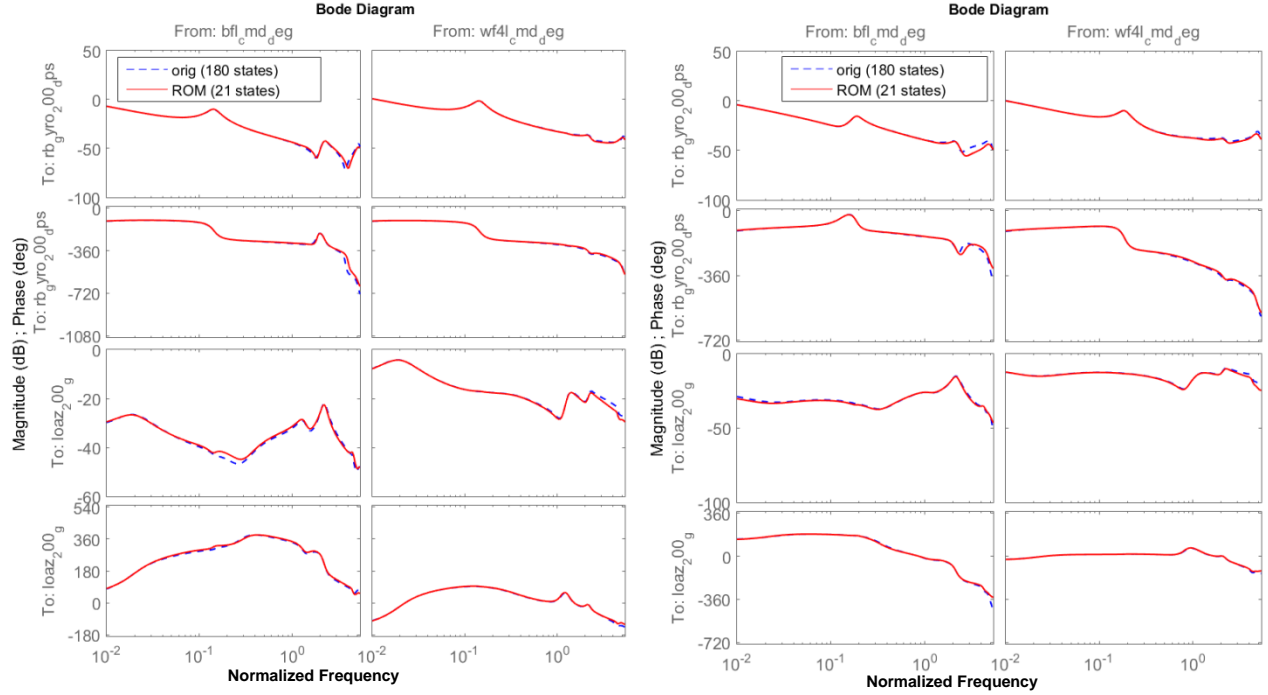
C   ROM with Different Flight Parameters

A desired feature that will saliently enhance the utility of MOR for aircraft ASE analysis and controller synthesis is its robustness and consistence of model configuration parameters regardless of the flight conditions. A thorough study to investigate the effect of varying flight parameters (KEAS and fuel weights) on MOR performance was also carried out. In the MOR analysis below, models with different flight parameters (KEAS = 70 or fuel weight of 78 lbs) from the benchmark case (100 KEAS and fuel weight of 10 lbs) were interrogated. Note that all the modeling configuration parameters (number of states/dimensions to keep or truncate) at each step remained the same as the case study in Section A above. Figure 7 illustrate the overall comparison of the magnitude and phase in the frequency domain between the full-order X-56A model and the ROM with 21 states for the non-benchmark cases. It shows that the ROMs at the new flight conditions are still able to accurately capture the dynamics in all input-output channels in the entire frequency range of interest for control design. The minor deviation of ROM from the full-order model only occurs at the middle-to-high frequency regime. The excellent ROM performance at various flight conditions substantiates pronounced robustness and utility of our MOR methods.
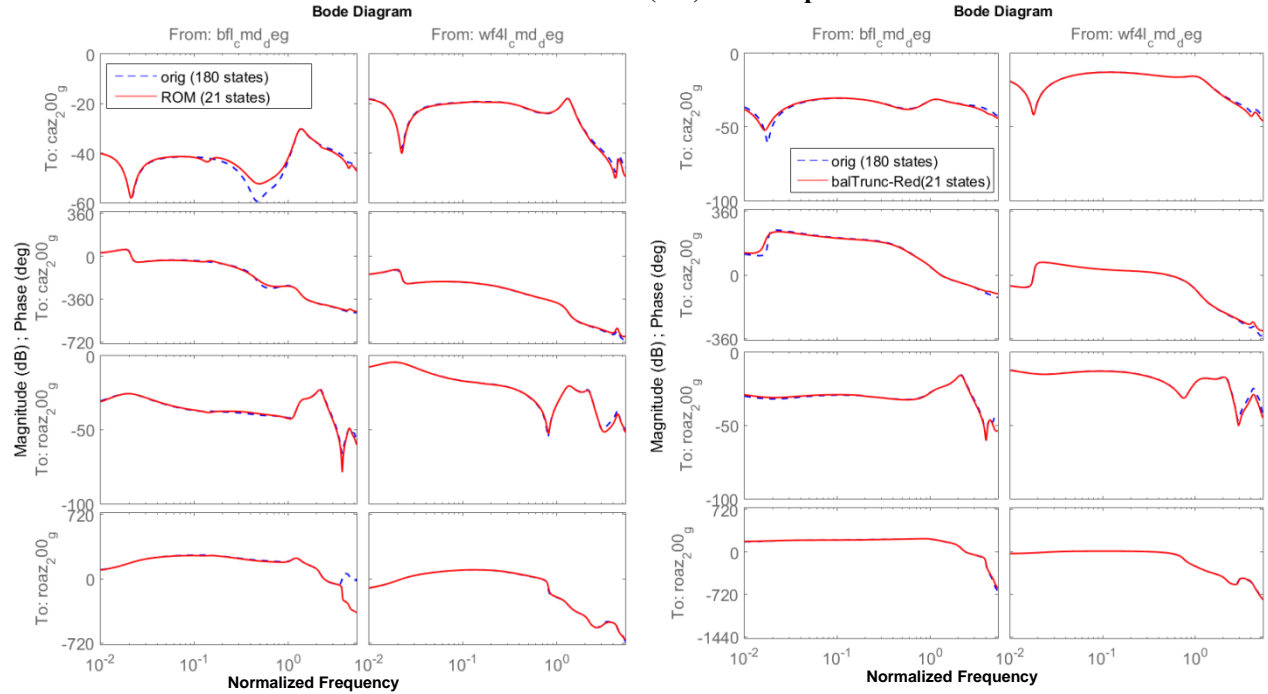

(a-1) From Inputs to q and p   **(b-1) From Inputs to q and p**

(a-2) From Inputs to r and ASESNSR600

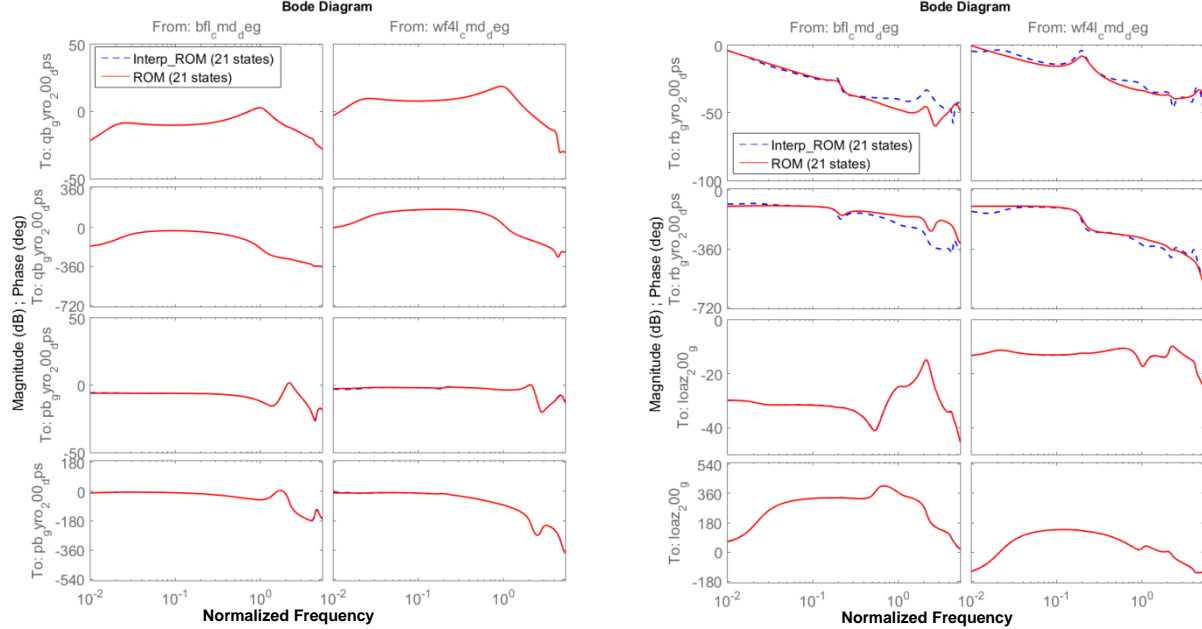**(b-2) From Inputs to r and ASESNSR600**

(a-3) From Inputs to ASESNSR1000 and ASESNSR1300

(b-3) From Inputs to ASESNSR1000 and ASESNSR1300

Figure 7. Comparison in magnitude and phase in the frequency domain between the full-order X-56A model (180 states) and the ROM. From Inputs: bfl_cmd_deg (BFL) and wf4l_cmd_deg (WF4L); To outputs: qb_gyro_200_dps (q), pb_gyro_200_dps (p), rb_gyro_200_dps (r), loaz_200_g (ASESNSR600), caaz_200_g (ASESNSR1000), and roaz_200_g (ASESNSR1300). (a) 70 KEAS and fuel weight of 10 lbs; and (b) 100 KEAS and fuel weight of 78 lbs.
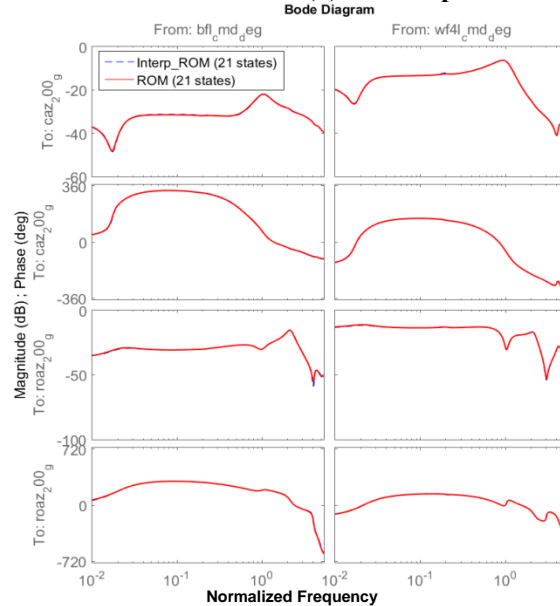
D ROM Interpolation

The consistent state representation and ROM interpolation based on common subspace reprojection and linear matrix interpolation as formulated above was also investigated. Figure 8 portrays the comparison of the ROMs at KEAS = 102 attained by two means: the first one (labeled as "ROM") was constructed by directly reducing the original, full-order X-56A model at KEAS = 102, and the second (labeled as "Interp ROM") by interpolating two ROMs obtained at KEAS = 100 and 104. Both ROMs agree with each other very well in predicting the vehicle dynamics. Figure 8b exhibits minor difference between the two ROMs in the channel from the BFL actuator to the yaw rate sensor (*r*) at the middle-to-high frequency regime. It may be attributed to the nonlinear dependence of system matrices on the flight parameters or the unbalanced input/output channels, and will be investigated in future.

(a) From Inputs to q and p

(b) From Inputs to r and ASESNSR 600

(c) From Inputs to ASESNSR1000 and ASESNSR1300

Figure 8. Comparison in magnitude and phase in the frequency domain between ROM obtained by MOR of the full-order X-56A model and the interpolated ROM. From Inputs: bfl_cmd_deg (BFL) and wf4l_cmd_deg (WF4L); To outputs: qb_gyro_200_dps (q), pb_gyro_200_dps (p), rb_gyro_200_dps (r), loaz_200_g (ASESNSR600), caaz_200_g (ASESNSR1000), and roaz_200_g (ASESNSR1300).

VI. Conclusion

This paper presented a holistic model order reduction (MOR) framework for constructing high-quality linear parameter-varying aeroservoelastic reduced order models (ASE-ROMs) of flexible aircraft. Key MOR modules of sequential model reduction, consistent model representation, and model interpolation have been established to streamline the workflow. A suite of proven model reduction techniques, including truncation and residualization, modal reduction, and balanced realization and truncation have been developed to determine optimal ROMs at grid points across the flight envelope. A novel method combing singular value decomposition and common subspace projection has been developed to unify the state representation for the ROMs obtained from non-orthonormal transformation-based MOR. Parameter-weighted matrix interpolation has been carried out to construct a globally functional LPV ASE ROM. The developed MOR technology has been applied to the X-56A MUTT vehicle with flexible wing to examine its capability of generating reliable ROMs for control design. Our studies demonstrate that the X-56A ROM was able to accurately describe vehicles dynamics and input/output response at various flight conditions in the practically important frequency regime while the number of states in ROM was reduced by 10X. The technology enables robust ASE controller synthesis for aircraft and novel vehicle design for flutter suppression and gust load alleviation

Acknowledgments

References

1.   Pak, C. and S. Lung, *Flutter Analysis of Aerostructures Test Wing with Test Validated Structural Dynamic Model.* Journal of aircraft, 2011. **48**(4): p. 1263-1272.
2.   Sheta, E.F., et al., *Computational and experimental investigation of limit cycle oscillations of nonlinear aeroelastic systems.* Journal of Aircraft, 2002. **39**(1): p. 133-141.
3.   Silva, W., et al. *Development of Aeroservoelastic Analytical Models and Gust Load Alleviation Control Laws of a SensorCraft Wind- Tunnel Model Using Measured Data.* in *47th AIAA/ASME/ASCE/AHS/ASC Structures, Structural Dynamics, and Materials Conference*. 2006.
4.   Hjartarson, A., P.J. Seiler, and G.J. Balas. *Lpv aeroservoelastic control using the lpvtools toolbox.* in *AIAA Atmospheric Flight Mechanics (AFM) Conference*. 2013.
5.   Theis, J., et al. *Modal Matching for LPV Model Reduction of Aeroservoelastic Vehicles.* in *AIAA Atmospheric Flight Mechanics Conference*. 2015. Kissimmee, Florida.
6.   Poussot-Vassal, C. and C. Roos. *Flexible aircraft reduced-order LPV model generation from a set of large-scale LTI models.* in *American Control Conference (ACC), 2011*. 2011. IEEE.
7.   Moreno, C.P., P.J. Seiler, and G.J. Balas, *Model Reduction for Aeroservoelastic Systems.* Journal of Aircraft, 2014. **51**(1): p. 280-290.
8.   Panzer, H., et al., *Parametric model order reduction by matrix interpolation.* at-Automatisierungstechnik Methoden und Anwendungen der Steuerungs-, Regelungs-und Informationstechnik, 2010. **58**(8): p. 475-484.
9.   *http://www.zonatech.com/ZAERO.htm*.
10.   *http://www.mscsoftware.com/product/msc-nastran*.
11.   Adegas, F.D., et al. *Reduced-order LPV model of flexible wind turbines from high fidelity aeroelastic codes.* in *Control Applications (CCA), 2013 IEEE International Conference on*. 2013. IEEE.
12.   Pak, C.-g. and S. Truong. *Creating a Test Validated Structural Dynamic Finite Element Model of the X-56A Aircraft.* in *5TH AIAA/ISSMO MULTIDISCIPLINARY ANALYSIS AND OPTIMIZATION CONFERENCE*. 2014.
13.   Hjartarson, A., P.J. Seiler, and G.J. Balas. *Lpv aeroservoelastic control using the lpvtools toolbox.* in *AIAA Atmospheric Flight Mechanics (AFM) Conference*. 2013.